Acta Crystallographica Section B
Structural Science
ISSN 0108-7681

Relation between photochromic properties and molecular structures in salicylideneaniline crystals

Kohei Johmoto,[a]* Takashi Ishida,[a] Akiko Sekine,[a] Hidehiro Uekusa[a] and Yuji Ohashi[a,b]

[a]Department of Chemistry and Material Science, Tokyo Institute of Technology, O-okayama, Meguro-ku, Tokyo 153-8902, Japan, and [b]Ibaraki Quantum Beam Research Center, Shirakata, Tokai, Ibaraki 319-1106, Japan

Correspondence e-mail: johmoto@chem.titech.ac.jp

Received 10 January 2012
Accepted 13 March 2012

The crystal structures of the salicylideneaniline derivatives *N*-salicylidene-4-*tert*-butyl-aniline (1), *N*-3,5-di-*tert*-butyl-salicylidene-3-methoxyaniline (2), *N*-3,5-di-*tert*-butyl-salicylidene-3-bromoaniline (3), *N*-3,5-di-*tert*-butyl-salicylidene-3-chloroaniline (4), *N*-3,5-di-*tert*-butyl-salicylidene-4-bromoaniline (5), *N*-3,5-di-*tert*-butyl-salicylidene-aniline (6), *N*-3,5-di-*tert*-butyl-salicylidene-4-carboxyaniline (7) and *N*-salicylidene-2-chloroaniline (8) were analyzed by X-ray diffraction analysis at ambient temperature to investigate the relationship between their photochromic properties and molecular structures. A clear correlation between photochromism and the dihedral angle of the two benzene rings in the salicylideneaniline derivatives was observed. Crystals with dihedral angles less than 20° were non-photochromic, whereas those with dihedral angles greater than 30° were photochromic. Crystals with dihedral angles between 20 and 30° could be either photochromic or non-photochromic. Inhibition of the pedal motion by intra- or intermolecular steric hindrance, however, can result in non-photochromic behaviour even if the dihedral angle is larger than 30°.

1. Introduction

Photochromic compounds undergo reversible colour changes upon photoirradiation as a consequence of an associated chemical transformation. This in turn leads to changes in the physicochemical properties of such compounds including absorption, fluorescence, refraction index and electric permittivity (Duerr & Bouas-Laurent, 1990; Crano & Guglielmetti, 1999). Photochromic compounds have attracted considerable attention because of their application in a variety of areas including photochromic lenses (Armistead & Stookey, 1964), rewritable papers (Sousa & Kashnow, 1969), photo-switching materials (Fukaminato *et al.*, 2004), optical data storages (Kawata & Kawata, 2000) and biological sensors (Mizuno *et al.*, 2008).

Salicylideneaniline (SA) derivatives are well known as photochromic compounds, undergoing a colour change from yellow to red upon irradiation with UV light and the reverse colour change upon exposure to visible light or heat (thermal fading). These compounds can be readily synthesized according to a procedure first reported in 1909, involving the condensation reaction of salicylaldehydes and anilines (Senir & Shepheard, 1909; Senir *et al.*, 1912). Furthermore, SA derivatives have demonstrated a high resistance to fatigue and this is an important property for any prospective photochromic compound to have (Andes & Manikowski, 1968). Following a systematic investigation into the relationship between the structural and physical properties of SA derivatives, it was proposed that crystals with a non-planar molecular

conformation would exhibit photochromic properties and that those with a planar molecular conformation would be non-photochromic and exhibit thermochromic properties (Cohen & Schmidt, 1962). Further consideration later led to the assertion that photochromic and thermochromic properties were mutually exclusive (Cohen, Hirshberg & Schmidt, 1964; Cohen, Schmidt & Flavian, 1964; Bregman *et al.*, 1964; refcode CHILSAN). More recently, however, it was revealed that, as a consequence of tautomerization between the enol and *cis*-keto forms, the majority of SA derivatives have thermochromic properties, regardless of their photochromic properties (Ogawa *et al.*, 1998; Fujiwara *et al.*, 2004; Harada *et al.*, 2007).

In light of the many controversies surrounding the understanding of photochromic properties (Duerr & Bouas-Laurent, 1990), we clearly demonstrated that the metastable red-coloured species in photo-irradiated SA crystals takes the *trans*-keto form (Harada *et al.*, 1999) by X-ray crystal structure analysis using two-photon excitation. Thus, from a mechanistic perspective, this provided an illustration that photochromism involves the transfer of a proton from the phenolic OH group of the enol form to the N atom of the imine group, generating the *cis*-keto form that is subsequently converted into the red-coloured *trans*-keto form, as shown in Scheme 1. Since the photochromic molecular transformation from enol to *trans*-keto forms occurs without destroying the single-crystal form, it was assumed that the transformation occurs *via* pedal motion in a manner similar to the thermal motion of azobenzene crystals (Harada *et al.*, 1997; Harada & Ogawa, 2009), which is known as a space-efficient motion in crystals.

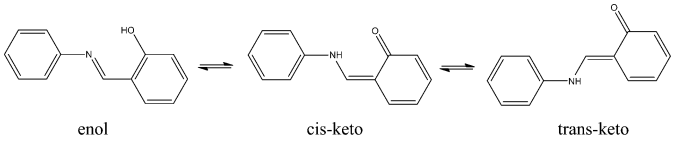

Scheme 1

Furthermore, there is no consistency in the thermal fading reaction rates of SA derivatives from the red-coloured *trans*-keto form to the original pale-yellow enol form. In a recent publication, we clearly demonstrated using keto-form structures of polymorphic crystals that thermal fading reaction rates were dependent upon intermolecular hydrogen bonding between the NH group of the *trans*-keto form and hydrogen-bond acceptors on neighbouring molecules (Johmoto *et al.*, 2009). These results were in good agreement with the *ab initio* calculation (Mikami & Nakamura, 2004).

Although it has long been accepted that molecular planarity plays an important role in photochromic reactions, there have been few reports investigating threshold values for the planarity (Haneda *et al.*, 2007). Furthermore, several SA derivatives with dihedral angles of approximately 90° have recently been reported that did not exhibit photochromism (Fukuda *et al.*, 2003). Given the range of conflicting experimental information and opinion, further investigation into the relationship between the planar conformations of SA derivatives and their photochromic properties is required. In this study we report the crystal structures of eight SA derivatives to obtain a quantitative threshold value relating the non-planarity of SA crystals to the occurrence of photochromic and non-photochromic behaviour. The SA crystals reported so far in the literature were also included in the study.

2. Experimental

2.1. Preparation of salicylideneaniline derivatives

Salicylaldehyde (1.0 mmol) and aniline (1.0 mmol) were dissolved in methanol (50 ml) at 298 K. The resulting solution was stirred for 10 min and evaporated under reduced pressure until the crude condensation product was precipitated from solution and collected by filtration. Pure crystals were obtained by recrystallization from ethanol at 298 K. The salicylideneanilines (1)–(8) were obtained according to the same methodology by condensation of the corresponding salicylaldehydes and anilines, which have the substituents corresponding to the final products (Scheme 2).

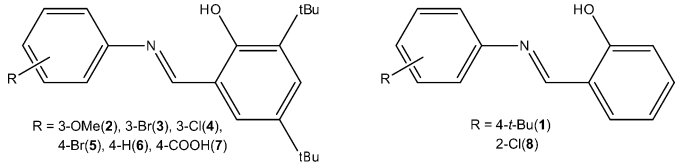

Scheme 2

2.2. Identification of photochromism by UV–vis spectrum

The UV–vis spectra of the SA crystals were measured at 298 K with a JASCO V-560 spectrometer equipped with the option (ISV-469) for diffuse reflectance spectroscopy. Analytical samples were prepared by mixing the SA crystals (7 mg) with $BaSO_4$ powder (350 mg). Photoirradiation was carried out through a glass filter (HOYA UV360) at 298 K with a high-pressure Hg lamp transmitting at a wavelength of 365 nm. Measurements were taken before and after photoirradiation.

2.3. Single-crystal X-ray diffraction analysis

Single-crystal X-ray diffraction data were collected at ambient temperature in ω-scan mode with R-AXIS RAPID and R-AXIS RAPID II imaging plate cameras (Rigaku) using graphite-monochromated Mo $K\alpha$ radiation (λ = 0.71075 Å) obtained from a rotating anode source and Cu $K\alpha$ radiation (λ = 1.54186 Å) from a rotating anode source with a confocal multilayer mirror. The data were collected at ambient temperature to correspond with the conditions of the photochromic reaction. The integrated and scaled data were empirically corrected for absorption effects with *ABSCOR* (Higashi, 1995). The initial structures were solved by direct methods with *SHELXS*97 (Sheldrick, 2008) and refined on F_0^2 with *SHELXL*97 (Sheldrick, 2008). With the exception of the disordered C atoms of the *tert*-butyl group, the non-H atoms were refined anisotropically, and all of the H atoms were obtained geometrically and included in the calculations using the riding atom model. The dihedral angles between the two benzene rings of SA molecules were calculated using *SHELXL*97 (Sheldrick, 2008). Although a crystal structure for

Table 1
Experimental details.

For all structures: $Z = 4$. H-atom parameters were constrained.

	(1)	(2)	(3)	(4)
Crystal data				
Chemical formula	$C_{17.12}H_{19.35}NO$	$C_{22}H_{29}NO_2$	$C_{21}H_{26}BrNO$	$C_{21}H_{26}ClNO$
M_r	255.13	339.46	388.34	343.88
Crystal system, space group	Monoclinic, P21/c	Triclinic, $P\overline{1}$	Triclinic, $P\overline{1}$	Triclinic, $P\overline{1}$
Temperature (K)	296	293	296	296
a, b, c (Å)	14.3711 (8), 6.4227 (4), 17.9938 (9)	10.814 (2), 12.011 (2), 15.727 (3)	10.7505 (6), 11.5008 (7), 16.3284 (8)	10.7392 (12), 11.5369 (15), 16.1292 (19)
α, β, γ (°)	90, 116.819 (4), 90	89.25 (3), 81.21 (3), 89.97 (3)	87.9590 (10), 83.166 (2), 89.536 (2)	88.032 (3), 82.446 (3), 89.642 (3)
V (Å^3)	1482.20 (14)	2018.7 (7)	2003.20 (19)	1979.8 (4)
$F(000)$	544	736	808	7364
D_x (Mg m^{-3})	1.135	1.117	1.288	1.154
Radiation type	Mo $K\alpha$	Mo $K\alpha$	Mo $K\alpha$	Mo $K\alpha$
μ (mm^{-1})	0.07	0.07	2.06	0.20
Crystal size (mm)	0.34 × 0.30 × 0.18	0.34 × 0.26 × 0.06	0.18 × 0.17 × 0.04	0.15 × 0.07 × 0.03
Data collection				
Diffractometer	Rigaku R-AXIS RAPID IP area detector	Bruker SMART CCD area detector	Rigaku R-AXIS RAPID IP area detector	Rigaku R-AXIS RAPID IP area detector
Absorption correction	Multi-scan, absorption was corrected by *ABSCOR*	Multi-scan, absorption was corrected by *SADABS*	Multi-scan, absorption was corrected by *ABSCOR*	Multi-scan, absorption was corrected by *ABSCOR*
T_{min}, T_{max}	0.885, 0.988	0.976, 0.996	0.189, 0.928	0.729, 0.994
No. of measured, independent and observed [$I > 2\sigma(I)$] reflections	23 765, 3381, 2187	29 048, 10 049, 5423	19 830, 9015, 4719	16 014, 7172, 2946
R_{int}	0.036	0.036	0.054	0.079
θ values (°)	$\theta_{max} = 27.5$, $\theta_{min} = 3.0$	$\theta_{max} = 28.4$, $\theta_{min} = 1.3$	$\theta_{max} = 27.4$, $\theta_{min} = 3.0$	$\theta_{max} = 25.3$, $\theta_{min} = 3.0$
$(\sin\theta/\lambda)_{max}$ (Å^{-1})	0.649	0.668	0.648	0.602
Completeness to θ	99.5% for 27.48°	99.5% for 28.35°	98.9% for 27.43°	99.1% for 25.34°
Refinement				
$R[F^2 > 2\sigma(F^2)]$, $wR(F^2)$, S	0.057, 0.190, 1.13	0.044, 0.128, 0.92	0.043, 0.143, 1.08	0.064, 0.164, 1.02
No. of reflections	3381	10 049	9015	7172
No. of parameters	194	482	445	461
No. of restraints	0	0	0	0
$\Delta\rho_{max}$, $\Delta\rho_{min}$ (e Å^{-3})	0.22, −0.21	0.24, −0.16	0.87, −0.78	0.20, −0.19
Extinction method	*SHELXL*	*SHELXL*	None	None
Extinction coefficient	0.023 (4)	0.0230 (19)	–	–

	(5)	(6)	(7)	(8)
Crystal data				
Chemical formula	$C_{21.05}H_{26.14}BrNO$	$C_{21}H_{27}NO$	$C_{22}H_{27}NO_3$	$C_{13}H_{10}ClNO$
M_r	388.34	309.44	353.45	231.67
Crystal system, space group	Monoclinic, $P2_1/c$	Orthorhombic, $Pna2_1$	Monoclinic, $P2_1/c$	Monoclinic, $P2_1/c$
Temperature (K)	296	296	293	293
a, b, c (Å)	18.0699 (14), 10.5997 (10), 10.3838 (9)	12.4043 (6), 8.9918 (5), 16.6903 (7)	6.1482 (4), 19.5491 (13), 17.0976 (13)	4.6868 (1), 18.9497 (4), 12.8231 (2)
β (°)	92.858 (2)	90	109.453 (3)	105.9680 (10)
V (Å^3)	1986.4 (3)	1861.59 (16)	1937.7 (2)	1094.92 (4)
$F(000)$	808	672	760	480
D_x (Mg m^{-3})	1.299	1.104	1.212	1.405
Radiation type	Mo $K\alpha$	Mo $K\alpha$	Mo $K\alpha$	Mo $K\alpha$
μ (mm^{-1})	2.08	0.07	0.08	2.88
Crystal size (mm)	0.20 × 0.14 × 0.06	0.50 × 0.35 × 0.15	0.40 × 0.30 × 0.02	0.33 × 0.10 × 0.06
Data collection				
Diffractometer	Rigaku R-AXIS RAPID IP area detector	Rigaku R-AXIS RAPID IP area detector	Rigaku R-AXIS RAPID IP area detector	Rigaku VM-SPIDER IP area detector
Absorption correction	Multi-scan, absorption was corrected by *ABSCOR*	Multi-scan, absorption was corrected by *ABSCOR*	Multi-scan, absorption was corrected by *ABSCOR*	Multi-scan, absorption was corrected by *ABSCOR*
T_{min}, T_{max}	0.559, 0.884	0.798, 0.990	0.627, 0.998	0.340, 0.837
No. of measured, independent and observed [$I > 2\sigma(I)$] reflections	18 792, 4500, 1915	17 422, 2193, 1955	17 354, 4410, 2938	12 241, 1976, 1565
R_{int}	0.109	0.032	0.087	0.046
θ values (°)	$\theta_{max} = 27.5$, $\theta_{min} = 3.0$	$\theta_{max} = 27.4$, $\theta_{min} = 3.1$	$\theta_{max} = 27.5$, $\theta_{min} = 2.1$	$\theta_{max} = 68.2$, $\theta_{min} = 4.3$

Table 1 (continued)

	(5)	(6)	(7)	(8)
$(\sin\theta/\lambda)_{max}$ (Å^{-1})	0.649	0.648	0.649	0.602
Completeness to θ	99.0% for 27.46°	99.8% for 27.42°	98.9% for 27.43°	98.3% for 68.22°
Refinement				
$R[F^2 > 2\sigma(F^2)]$, $wR(F^2)$, S	0.059, 0.147, 1.02	0.039, 0.101, 1.06	0.072, 0.206, 1.03	0.056, 0.170, 1.08
No. of reflections	4500	2193	4410	1976
No. of parameters	241	214	272	145
No. of restraints	1	1	0	0
$\Delta\rho_{max}$, $\Delta\rho_{min}$ (e Å^{-3})	0.30, −0.38	0.22, −0.14	0.33, −0.27	0.33, −0.21

Computer programs used: *PROCESS-AUTO* (Rigaku, 1998), *SMART* (Siemens, 1996), *SAINT* (Siemens, 1994*a*), *SADABS* (Sheldrick, 1996), *SHELXL*97, *SHELXS*97 (Sheldrick, 2008), *ORTEP*3 (Farrugia, 2008), *SHELXTL* (Siemens, 1994*b*).

(6) had already been reported at 223 K (Ahmad *et al.*, 2011), in the interest of consistency and direct comparison the structure was also analysed at ambient temperature. The crystallographic data and experimental details are summarized in Table 1.

3. Results

3.1. Crystal and molecular structures before photoirradiation

The molecular and crystal structures of (1) are shown in Figs. 1 and 2. The *tert*-butyl group of (1) is disordered and can exist in three different conformations. The conformation with the largest occupancy is depicted. There is a strong intramolecular hydrogen bond of O1—H···N1, occurring over a short O1···N1 distance of 2.612 (2) Å. This leads to the observed planar conformation in the O1—C2—C1—C7—N1 moiety. The torsion angles of the C2—C1—C7—N1 and C1—C7—N1—C8 moieties are 5.7 (3) and −178.8 (2)°. However, the torsion angle of C7—N1—C8—C9 is significantly large, 43.5 (3)°, leading to the large observed dihedral angle of 49.12 (7)° between the two terminal benzene rings. No unusually short contacts were observed in the crystal structure and the loose contacts between the *tert*-butyl groups of neighbouring molecules led to the disordered structure of the group. The crystals of (2)–(4) were composed of two crystallographically independent molecules, *A* and *B*, in their unit cells. The molecular structures of (2*A*), (2*B*), (3*A*), (3*B*), (4*A*), (4*B*) and (5) were found to be similar to that of (1), with the corresponding dihedral angles between the two benzene rings observed to be 48.44 (6), 46.40 (6), 45.07 (12), 45.29 (12), 44.37 (15), 44.66 (14) and 27.25 (19)°. The molecular structure of (6) is shown in Fig. 3. The bond distances and angles, the intramolecular hydrogen-bond distance and the torsion angles of the C2—C1—C7—N1 and C1—C7—N1—C8 moieties were found to be similar to those observed in the crystal structures

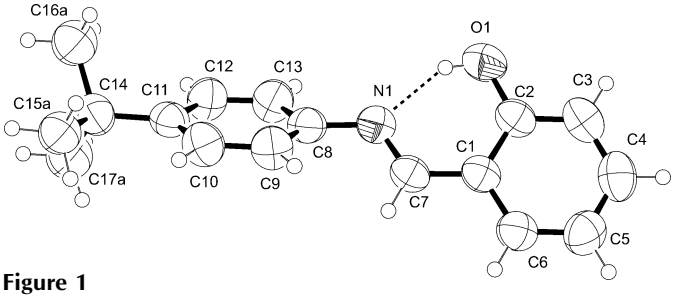

Figure 1
Molecular structure of *N*-salicylidene-4-*tert*-butylaniline (1). The displacement ellipsoids are drawn at the 50% probability level. The hydrogen bond is drawn in a dotted line. The *tert*-butyl group with the highest occupancy is shown.

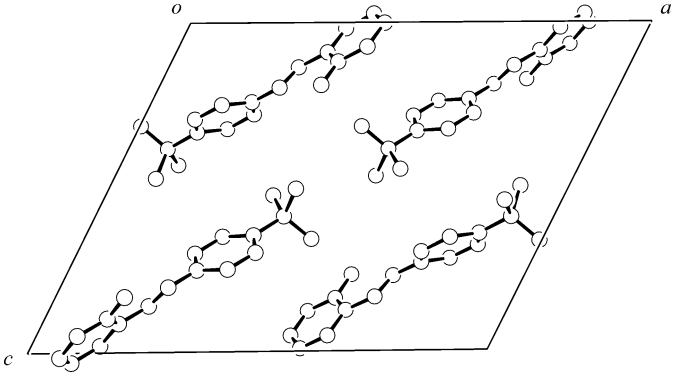

Figure 2
Crystal structure of *N*-salicylidene-4-*tert*-butylaniline (1) viewed along the *b* axis. H atoms are omitted for clarity.

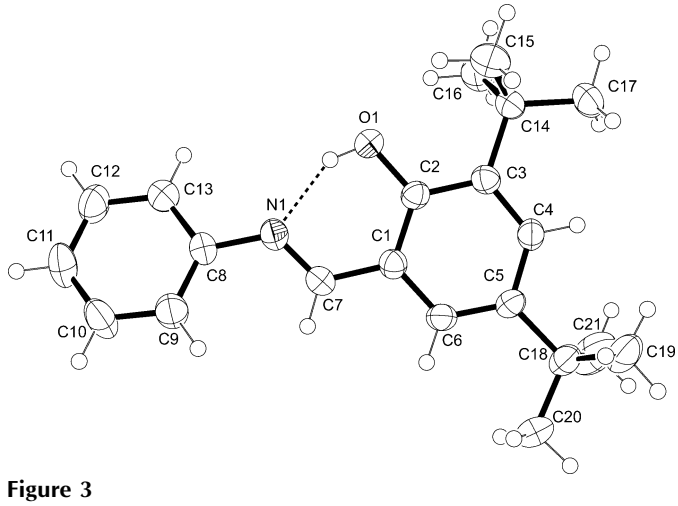

Figure 3
Molecular structure of *N*-3,5-di-*tert*-butylsalicylideneaniline (6). The displacement ellipsoids are drawn at the 50% probability level. The hydrogen bond is drawn as a dotted line.

of (1)–(5). Both the torsion angle of the C7—N1—C8—C9 moiety and the dihedral angle between the two terminal benzene rings, however, were found to be smaller at 25.0 (3) and 21.56 (12)°.

The molecular and crystal structures of (8) are shown in Figs. 4 and 5. The bond distances and angles were found to be as anticipated. A strong intramolecular hydrogen bond of O1—H···N1 was observed over a short O1···N1 distance of 2.621 (3) Å. Compound (8) was found to be whole planar. The torsion angles of the C2—C1—C7—N1, C1—C7—N1—C8 and C7—N1—C8—C9 moieties were −3.3 (5), −178.3 (3) and 2.0 (5)°, and the dihedral angle between the two benzene rings was found to be 2.82 (20)°. These planar molecules are stacked as a sheet along the *a* and *b* axes and the sheets themselves are stacked alternately along the *c* axis. The crystals of (7) were also revealed to be whole planar in structure, in a similar manner to that observed in (8). It has been reported that (8) can exist in another polymorphic form, (8′) (Bregman *et al.*, 1964; refcode CHILSAN). Whilst the reported crystal of (8′) reveals that the bond distances, bond angles and torsion angles of the C2—C1—C7—N1 and C1—C7—N1—C8 moieties are similar to those observed in (8), the aniline moiety of (8′) is twisted out of the plane resulting in the larger dihedral angle between the two terminal benzene rings of 51.1°. It is known that the *ortho* position atom of the aniline ring has an influence on the planarity in SA derivative molecules such as *N*-salicylidene-2-aminopyridine (Moustakali-Mavridis *et al.*, 1978, 1980), which is caused by the absence or presence of steric hindrance between azomethine H and the aniline ring. Similar hindrance would occur when the *ortho*-substituent is situated near the azomethine H. However, in this work the *ortho*-substituent of the aniline ring of (8) directs to the opposite direction to azomethine H. The only possible intramolecular interaction is between aniline and azomethine H atoms, which is expected for all *ortho*-, *meta*- and *para*-substituted SA molecules. Thus, it has almost equal influence on the molecular conformation among all mono-substituted SAs. The different dihedral angles in polymorphic crystals of (8) and (8′), as described above, clearly indicate that the molecular conformation is determined by the molecular packing and intermolecular interactions. The eight SA crystals with various dihedral angles in this study may be a good choice

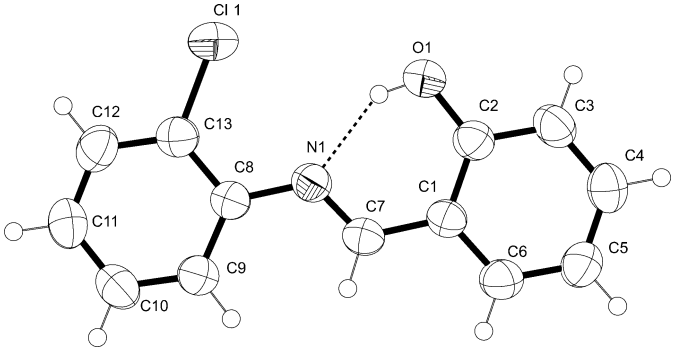

Figure 4
Molecular structure of *N*-salicylidene-2-chloroaniline (8). The displacement ellipsoids are drawn at the 50% probability level. The hydrogen bond is drawn as a dotted line.

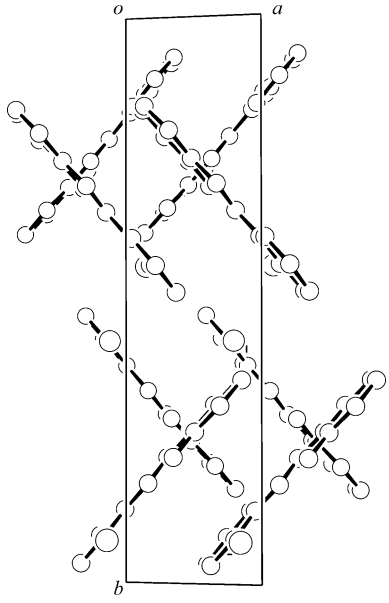

Figure 5
Crystal structure of *N*-salicylidene-2-chloroaniline (8) viewed along the *c* axis. H atoms are omitted for clarity.

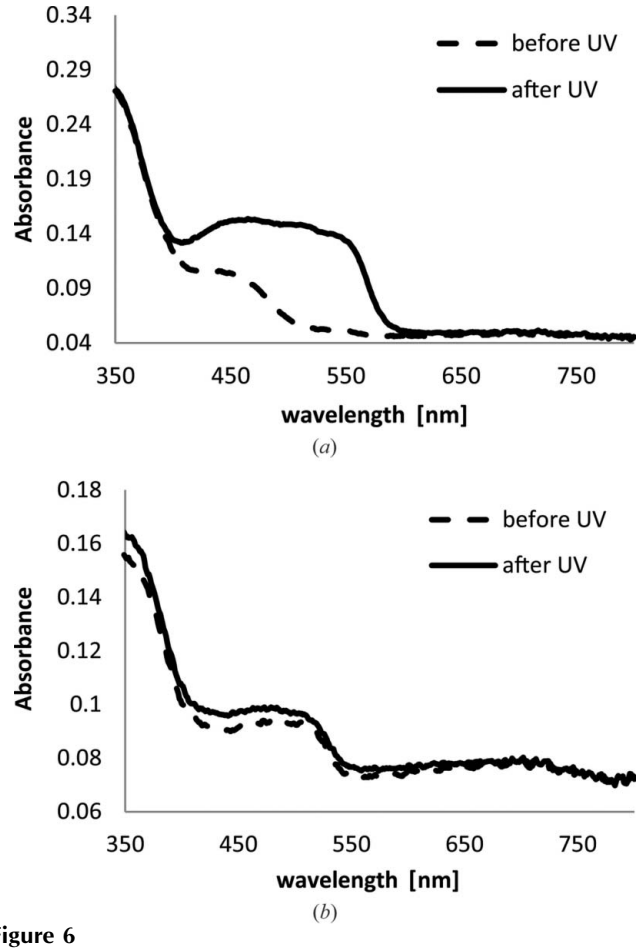

Figure 6
Reflectance spectra (*a*) for (1) and (*b*) for (8). Dashed and full curves indicate before and after photoirradiation.

Table 2
Selected bond distances (Å), angles, torsion angles and dihedral angles (°) of the SA derivatives (1)–(8) and (8′).

	(1)	(2*A*)†	(2*B*)†	(3*A*)†	(3*B*)†	(4*A*)†	(4*B*)†
O1—C2	1.350 (3)	1.357 (2)	1.358 (2)	1.359 (4)	1.350 (4)	1.358 (4)	1.360 (4)
C2—C1	1.408 (3)	1.410 (2)	1.412 (2)	1.413 (4)	1.406 (5)	1.415 (5)	1.412 (5)
C1—C7	1.450 (3)	1.450 (2)	1.453 (2)	1.452 (5)	1.457 (5)	1.449 (5)	1.447 (5)
C7—N1	1.280 (3)	1.284 (2)	1.283 (2)	1.278 (5)	1.271 (4)	1.281 (4)	1.280 (4)
N1—C8	1.421 (3)	1.420 (2)	1.424 (2)	1.420 (4)	1.420 (4)	1.429 (4)	1.424 (5)
N1···O1	2.612 (2)	2.582 (2)	2.608 (2)	2.580 (4)	2.596 (3)	2.599 (4)	2.578 (4)
C1—C7—N1	121.8 (2)	122.5 (1)	123.2 (1)	122.1 (3)	122.8 (3)	122.8 (3)	122.8 (3)
C7—N1—C8	120.4 (2)	121.1 (1)	119.9 (1)	121.0 (3)	120.6 (3)	119.8 (3)	120.8 (3)
C2—C1—C7—N1	5.7 (3)	−1.8 (2)	0.8 (2)	0.3 (5)	0.5 (5)	−0.3 (6)	1.5 (5)
C1—C7—N1—C8	−178.8 (2)	173.6 (1)	−173.1 (1)	−178.0 (3)	−177.4 (3)	178.5 (3)	−179.5 (3)
C7—N1—C8—C9	43.5 (3)	−46.2 (2)	45.4 (2)	45.4 (5)	46.1 (5)	−46.5 (5)	45.5 (5)
Dihedral angle (φ)	49.12 (7)	48.44 (6)	46.40 (6)	45.07 (12)	45.29 (12)	44.37 (15)	44.66 (14)

	(5)	(6)	(7)	(8)	(8′)	Average (1)–(8)
O1—C2	1.361 (5)	1.352 (2)	1.344 (2)	1.354 (3)	1.3709	1.356 (5)
C2—C1	1.394 (6)	1.409 (3)	1.401 (3)	1.402 (4)	1.3960	1.407 (6)
C1—C7	1.464 (6)	1.457 (3)	1.444 (3)	1.452 (5)	1.4563	1.453 (6)
C7—N1	1.278 (5)	1.279 (3)	1.266 (3)	1.276 (4)	1.2812	1.278 (5)
N1—C8	1.432 (5)	1.422 (2)	1.421 (3)	1.412 (4)	1.4272	1.423 (5)
N1···O1	2.621 (5)	2.563 (2)	2.610 (2)	2.621 (3)	2.614	2.599 (5)
C1—C7—N1	123.5 (4)	121.7 (2)	123.5 (2)	121.4 (3)	121.46	122.5 (4)
C7—N1—C8	119.6 (4)	123.4 (2)	121.0 (2)	121.8 (3)	118.62	120.7 (4)
C2—C1—C7—N1	−0.4 (7)	−2.5 (3)	−2.2 (4)	−3.3 (5)	−3.84	–
C1—C7—N1—C8	179.0 (4)	−179.9 (2)	−175.6 (2)	−178.3 (3)	175.07	–
C7—N1—C8—C9	27.5 (6)	25.0 (3)	7.7 (4)	2.0 (5)	−46.99	–
Dihedral angle (φ)	27.25 (19)	21.56 (12)	8.74 (12)	2.82 (20)	51.1	–

† (2*A*), (2*B*), (3*A*), (3*B*), (4*A*) and (4*B*) are crystallographically independent molecules.

to discuss the relationship between the structures and photochromic characters, although the intramolecular hindrance may be an important factor to govern the relationship for the di-*ortho*-substituted SA crystals, which will be discussed in the following section.

3.2. Photochromic reactivity

The UV–vis absorption spectra for crystals of (1) and (8) are shown in Figs. 6(*a*) and (*b*). Following the photoirradiation of (1), a significant difference was observed in the spectrum between 400 and 600 nm. Spectral changes similar to those observed in (1) also occurred for crystals of (2)–(5) in the range 450–550 nm. In contrast to these observations, photoirradiation of (8) did not result in any discernible difference and the spectrum remained unchanged. Crystals of (6) and (7) also behaved in the same way as (8). This indicated that the crystals of (1)–(5) were photochromic and that those of (6)–(8) were non-photochromic. Interestingly, crystals of (8′), another polymorphic form of (8), were reported to be photochromic (Bregman *et al.*, 1964; refcode CHILSAN).

4. Discussion

The selected bond distances, bond angles, intramolecular hydrogen-bond lengths, torsion angles of the C2—C1—C7—N1, C1—C7—N1—C8 and C7—N1—C8—C9 moieties and the dihedral angles of the two benzene rings of (1)–(8) are summarized in Table 2. Each parameter is averaged across the 11 molecules except for the torsion angle of the C7—N1—C8—C9 moiety and the dihedral angle. The corresponding distances and angles are in good agreement with one another. The relation between the dihedral angles of the two terminal benzene rings and the photochromic properties is shown in Fig. 7. There are two polymorphic crystal forms, (8) and (8′), which are non-photochromic and photochromic, respectively. Previously we reported that the compound *N*-3,5-di-*tert*-butylsalicylideneaniline-3-carboxyaniline (9) could exist in one of three polymorphic crystal forms, α, β and γ. The crystals of (9α) and (9β) exhibit photochromism and had dihedral angles of 60.95 (4) and 37.34 (6)°, respectively, whereas crystals of (9γ) were non-photochromic and had a dihedral angle of 28.90 (4)°. From Fig. 7 it is clear that the threshold value of the dihedral angle in relation to the occurrence of photochromic behaviour is 20 to 30°.

Recently it was reported that the twisted SA derivatives substituted with either methyl or *tert*-butyl groups at both *ortho* positions of the aniline ring were non-photochromic in spite of their large dihedral angles of 63.5 and 82.9°. In contrast, it was also reported in the same publication that SA derivatives substituted with either ethyl or isopropyl groups at the two *ortho* positions of the aniline ring exhibited photochromism and had dihedral angles of 82.3 and 73.6° (Fukuda *et*

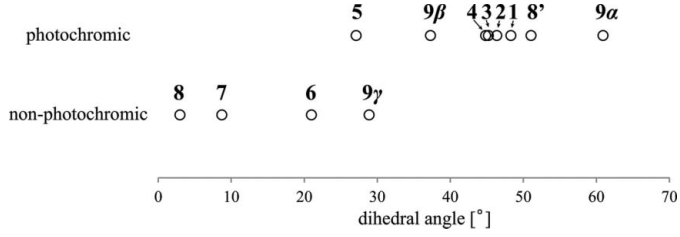

Figure 7
The relationship between photochromic properties and dihedral angles of SA derivatives. Each SA derivative corresponds to an open circle that indicates the photochromic property and the intramolecular dihedral angle between two benzene rings. The dihedral angles of SA derivative crystals are classified into photochromic (upper row) and non-photochromic (lower row) ones. Both types of photochromic and non-photochromic crystals are observed between 20 and 30°.

al., 2003). Based upon these observations, the authors claimed that crystal packing was responsible for the observed photochromic behaviour rather than the non-planarity of the molecules.

As discussed in the previous paper (Johmoto *et al.*, 2009), photochromism occurs as a consequence of a structural change between enol and *trans*-keto forms (Cohen & Schmidt, 1962; Cohen *et al.*, 1964; Harada *et al.*, 1999), which is schematically depicted in Fig. 8. During the transformation from the enol to the *trans*-keto form, the H atom bonded to the OH group is transferred to the N atom and the *cis*-keto form is produced. The central single —(H)N—C(H)— bond of the *cis*-keto form rotates by 180° around an axis connecting the two benzene rings. The benzene rings slide up and down maintaining the conformation. Given that this pedal-like motion does not lead to large movements in the peripheral atoms of the molecule, the crystal structure is sustained in the photochromic reaction. However, if both of the *ortho* positions of the aniline rings are substituted with *tert*-butyl groups, it is impossible for the conformation to change from the *cis*-keto to the *trans*-keto form due to steric repulsion between the *tert*-butyl groups and the H atoms of the methine and imino groups, as depicted in Fig. 9(*a*) in which the distances between the N atom and four methyl C atoms of the *tert*-butyl group close to the N atom were 2.870 (6) Å for N1···C28, 3.000 (7) Å for N1···C12, 3.224 (8) Å for N1···C11 and 3.509 (7) Å for N1···C27, respectively. In contrast, for SA derivatives substituted at both *ortho* positions of the aniline ring with isopropyl and ethyl groups, the pedal motion can still occur without intramolecular steric hindrance, as shown in Fig. 9(*b*), in which the distances between the N atom and four methyl C atoms of the iso-propyl group were 3.715 (7) Å for N2···C38, 3.838 (6) Å for N2···C31, 4.043 (5) Å for N2···C30

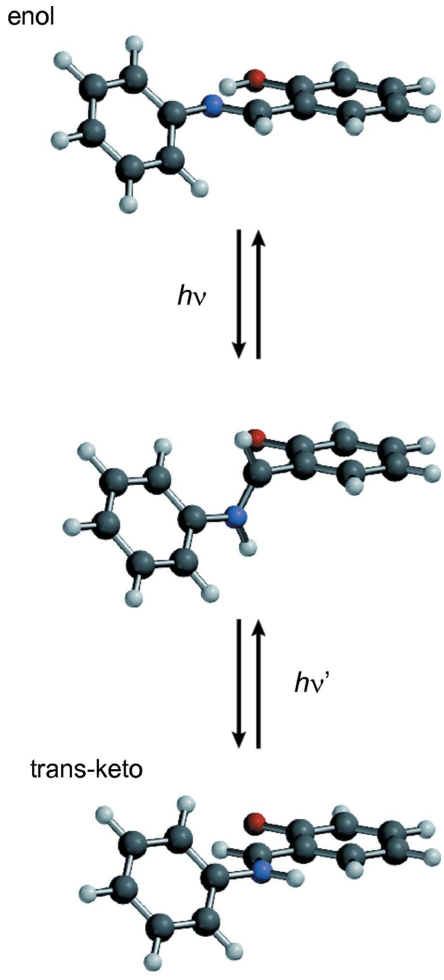

Figure 8
A schematic drawing of the pedal motion. Two benzene rings only move as pedals of a bicycle as the central NH—CH plane turns upside down in the transformation from enol to the *trans*-keto form.

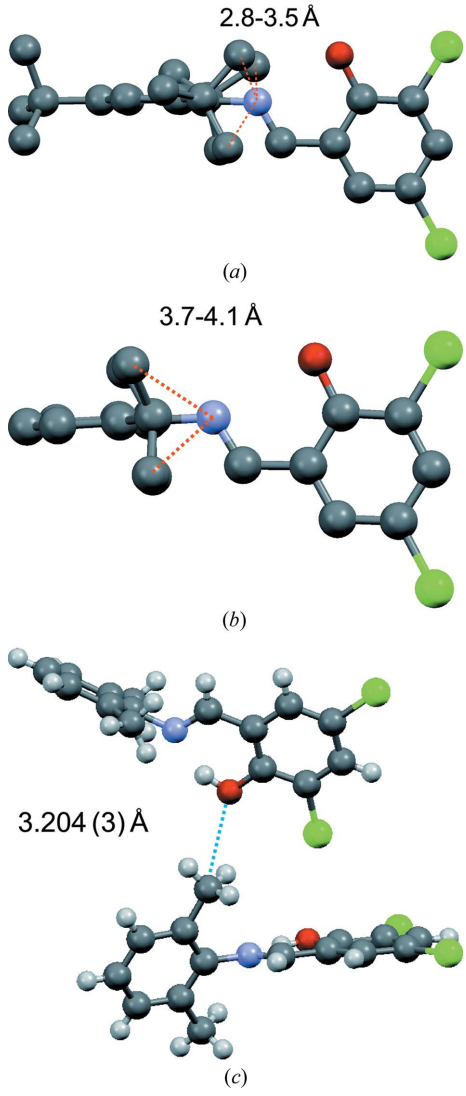

Figure 9
Schematic drawings of intramolecular steric hindrances for the SA molecules with (*a*) *ortho*-di-*tert*-butyl groups and (*b*) *ortho*-diisopropyl groups in the aniline rings. The distance ranges between the N atom and the nearest methyl C atoms of ^{i}Pr/^{t}Bu were included (Fukuda *et al.*, 2003). (*c*) Steric hindrance between the methyl group at the *ortho* position and the phenol group of the neighbouring molecule. There is an unusually short contact between the OH and the CH_3 groups in a non-photochromic crystal with *ortho*-dimethyl groups in the aniline rings, the C···O distance being 3.204 (3) Å (Fukuda *et al.*, 2003).

and 4.137 (5) Å for N2···C37. For SA derivatives substituted at both *ortho* positions of the aniline ring with methyl groups, there are both photochromic and non-photochromic crystals. For the photochromic crystals, pedal motion can easily occur as observed in the crystals with diisopropyl and diethyl groups. For the non-photochromic crystals, on the other hand, pedal motion appears to be restricted by the close contact of neighbouring molecules, as shown in Fig. 9(*c*). The slide motion of the benzene ring is hindered by the short intermolecular contact distance between the OH and CH_3 groups, where O···C is 3.204 (3) Å. Such a short contact is not observed in the crystal structures of (1)–(5) (the shortest intermolecular C···C, C···O, C···N distances being greater than 3.5 Å).

These observations clearly indicate that the non-planarity of the SA derivatives is necessary to initiate pedal motion; localizing the π-electrons into the two terminal benzene rings and the central CH═NH group. The threshold value for non-planarity resulting in photochromic behaviour is a dihedral angle of at least 30° between the two terminal benzene rings. However, the impact of intra- and intermolecular steric hindrance upon pedal motion inhibition represents an important factor in determining photochromism.

This work was supported by Grant-in-Aid for Scientific Research from the Japan Society for Promotion of Science.

References

Ahmad, J. U., Nieger, M., Sundberg, M. R., Leskela, M. & Repo, T. (2011). *J. Mol. Struct.* **995**, 9–19.

Andes, R. V. & Manikowski, D. M. (1968). *Appl. Opt.* **7**, 1179–1183.

Armistead, W. H. & Stookey, S. D. (1964). *Science*, **144**, 150–154.

Bregman, J., Leiserowitz, L. & Schmidt, G. M. (1964). *J. Chem. Soc.* pp. 2068–2085.

Cohen, M. D., Hirshberg, Y. & Schmidt, G. M. (1964). *J. Chem. Soc.* pp. 2051–2059.

Cohen, M. D. & Schmidt, G. M. (1962). *J. Chem. Phys.* **66**, 2442–2447.

Cohen, M. D., Schmidt, G. M. & Flavian, S. (1964). *J. Chem. Soc.* pp. 2041–2051.

Crano, J. C. & Guglielmetti, R. J. (1999). *Organic Photochromic and Thermochromic Compounds.* New York, London: Plenum Press.

Duerr, H. & Bouas-Laurent, H. (1990). *Photochromism Molecules and Systems.* Amsterdam: Elsevier.

Farrugia, L. J. (1997). *J. Appl. Cryst.* **30**, 565.

Fujiwara, T., Harada, J. & Ogawa, K. (2004). *J. Phys. Chem. B*, **108**, 4035–4038.

Fukaminato, T., Sasaki, T., Kawai, T., Tamai, N. & Irie, M. (2004). *J. Am. Chem. Soc.* **126**, 14843–14849.

Fukuda, H., Amimoto, K., Koyama, H. & Kawato, T. (2003). *Org. Biomol. Chem.* **1**, 1578–1583.

Haneda, T., Kawano, M., Kojima, T. & Fujita, M. (2007). *Angew. Chem. Int. Ed.* **46**, 6643–6645.

Harada, J., Fujiwara, T. & Ogawa, K. (2007). *J. Am. Chem. Soc.* **129**, 16216–16221.

Harada, J. & Ogawa, K. (2009). *Chem. Soc. Rev.* **38**, 2244–2252.

Harada, J., Ogawa, K. & Tomoda, S. (1997). *Acta Cryst.* B**53**, 662–672.

Harada, J., Uekusa, H. & Ohashi, Y. (1999). *J. Am. Chem. Soc.* **121**, 5809–5810.

Higashi, T. (1995). *ABSCOR*. Rigaku Corporation, Tokyo, Japan.

Johmoto, K., Sekine, A., Uekusa, H. & Ohashi, Y. (2009). *Bull. Chem. Soc. Jpn*, **82**, 50–57.

Kawata, S. & Kawata, Y. (2000). *Chem. Rev.* **100**, 1777–1788.

Mikami, M. & Nakamura, S. (2004). *Phys. Rev. B*, **69**, 134205.

Mizuno, H., Mal, T. K., Wälchli, M., Kikuchi, A., Fukano, T., Ando, R., Jeyakanthan, J., Taka, J. Shiro, Y., Ikura, M. & Miyawaki, A. (2008). *Proc. Natl Acad. Sci. USA*, **105**, 9927–9932.

Moustakali-Mavridis, I., Hadjoudis, E. & Mavridis, A. (1978). *Acta Cryst.* B**34**, 3709–3715.

Moustakali-Mavridis, I., Hadjoudis, B. & Mavridis, A. (1980). *Acta Cryst.* B**36**, 1126–1130.

Ogawa, K., Kasahara, Y., Ohtani, Y. & Harada, J. (1998). *J. Am. Chem. Soc.* **120**, 7107–7108.

Rigaku (1998). *PROCESS-AUTO*. Rigaku Corporation, Tokyo, Japan.

Senir, A. & Shepheard, F. G. (1909). *J. Chem. Soc. Trans.* **95**, 1943–1955.

Senir, A., Shepheard, F. G. & Clarke, R. (1912). *J. Chem. Soc. Trans.* **101**, 1950–1958.

Sheldrick, G. M. (1996). *SADABS*. University of Göttingen, Germany.

Sheldrick, G. M. (2008). *Acta Cryst.* A**64**, 112–122.

Siemens (1994*a*). *SAINT*. Siemens Analytical X-ray Instruments Inc., Madison, Wisconsin, USA.

Siemens (1994*b*). *SHELXTL*. Siemens Analytical X-ray Instruments Inc., Madison, Wisconsin, USA.

Siemens (1996). *SMART*. Siemens Analytical X-ray Instruments Inc., Madison, Wisconsin, USA.

Sousa, J. A. & Kashnow, R. A. (1969). *Rev. Sci. Instrum.* **40**, 966–967.